Characterization of Lanthanide(III) Ion Binding to Calmodulin Using Luminescence Spectroscopy†

Paul Mulqueen, Joel M. Tingey, and William DeW. Horrocks, Jr.*
Department of Chemistry, The Pennsylvania State University, University Park, Pennsylvania 16802
Received February 21, 1985

ABSTRACT: Pulsed dye laser excitation spectroscopy of the $^7F_0 \rightarrow {}^5D_0$ transition of Eu(III) reveals only a single peak as this ion is titrated into apocalmodulin. A titration based on the intensity of this transition shows that the first two Eu(III) ions bind quantitatively to two tight sites, followed by weaker binding (K_d = 2 μM) to two additional sites under conditions of high ionic strength (0.5 M KCl). This excitation experiment is also shown to be a general method for measuring contaminating levels of EDTA down to 0.2 μM in proton solutions. Experiments with Tb(III) using both direct laser excitation and indirect sensitization of Tb(III) luminescence through tyrosine residues in calmodulin also give evidence for two tight and two weaker binding sites (K_d = 2–3 μM). The indirect sensitization results primarily upon binding to the two weaker sites, implying that Tb(III) binds first to domains I and II, which are remote from tyrosine-containing domains III and IV. The $^7F_0 \rightarrow {}^5D_0$ excitation signal of Eu(III) was used to measure the relative overall affinities of the tripositive lanthanide ions, Ln(III), across the series. Ln(III) ions at the end of the series are found to bind more weakly than those at the beginning and middle of the series. Eu(III) excited-state lifetime measurements in H_2O and D_2O reveal that two water molecules are coordinated to the Eu(III) at each of the four metal ion binding sites. Measurements of Förster-type nonradiative energy-transfer efficiencies between Eu(III) and Nd(III) in the two tight sites were carried out by monitoring the excited-state lifetimes of Eu(III) in the presence and absence of the energy acceptor ion Nd(III). Measured energy-transfer efficiencies of 0.126 and 0.396 were obtained in H_2O and D_2O solutions, respectively. By use of a spectral overlap integral obtained from the absorption spectrum of Nd(III) bound in the two tight sites of calmodulin and a corrected emission spectrum for Eu(III) in calmodulin, a distance estimate of 12.1 ± 0.5 Å was obtained, with the H_2O and D_2O results agreeing to within 0.2 Å. This result supports a postulated structure for calmodulin based on its homology with parvalbumin.

Calmodulin, CaM,[1] a small (M_r 16 790), acidic (pI = 3.9–4.3) protein, serves as a universal intracellular sensor of the augmented cytosolic calcium ion concentration that follows cell stimulation [for reviews, see Cheung (1980a,b), Klee et al. (1980), Klee & Vanaman (1982), and Cormier (1983)]. CaM is capable of binding up to four calcium ions when the free calcium ion concentration rises to the ~10 μM level following the stimulating signal. A member of the class of calcium-modulated proteins (Kretsinger, 1980; Seamon & Kretsinger, 1983), CaM binds calcium ions in putative helix–loop–helix regions labeled I–IV, starting from the amino terminus. The binding of calcium ions triggers conformational changes in the protein that allow it to interact with and stimulate a raft of target enzymes. A detailed knowledge of the structure of CaM, its metal ion binding properties, the metal ion induced conformational changes, and its interaction with intracellular targets is central to an understanding of its mode of action.

There have been a large number of studies of Ca(II) ion binding to CaM (Haiech et al., 1981; Kohse & Heilmeyer, 1981; Cox et al., 1981; Burger et al., 1983; Potter et al., 1983; Cox, 1984) as well as of substitutional probes such as Cd(II) (Forsén et al., 1980; Andersson et al., 1982, 1983a,b), Gd(III) (Krebs & Carafoli, 1982), Tb(III) (Kilhoffer et al., 1980a,b; Wang et al., 1982; Wallace et al., 1982), and Eu(III) (Wang et al., 1982; Horrocks et al., 1983). Something less than universal agreement exists with regard to the values of the binding constants and the order (if any) with which various ions bind to the four sites. Furthermore, there is some question regarding the degree of metal ion loading required to produce a conformer capable of activating a particular enzyme.

The spectroscopic silence of the physiologically relevant Ca(II) ion has led us and others to explore the use of substitutional probe ions in the study of the structure, function, and metal ion binding properties of this important protein. In this paper the pulsed dye laser lanthanide ion, Ln(III), luminescence excitation technique developed in this laboratory (Horrocks & Sudnick, 1981), as well as tyrosine-sensitized Tb(III) luminescence, is employed to establish the sequence of Ln(III) ion binding and the nature of the binding sites. Although the three-dimensional structure of CaM remains unknown, our measurements of Förster-type nonradiative energy transfer between emissive [Eu(III)] and absorptive [Nd(III)] ions bound to CaM permits us to estimate the distance between the two tightest binding sites and provides support for a postulated structural model.

Materials and Methods

Calmodulin was purified from bovine testicles (Pel-Freeze, Inc.) with a method based on that described by Dedman & Kaetzel (1983). The detunicated testicles were homogenized in twice their volume of 25 mM Tris-HCl containing 1 mM EGTA (pH 7.5). The homogenate was heated rapidly to 80 °C in a microwave oven and immediately placed on ice. The

† This research was supported by National Institutes of Health Grant GM-23599.

[1] Abbreviations: CaM, calmodulin; Ln(III), trivalent lanthanide ions; EDTA, ethylenediaminetetraacetic acid; EGTA, [ethylenebis(oxyethylenenitrilo)]tetraacetic acid; Hepes, *N*-(2-hydroxyethyl)piperazine-*N*′-2-ethanesulfonic acid; Tris-HCl, tris(hydroxymethyl)aminomethane hydrochloride.

0006-2960/85/0424-6639$01.50/0

solution was clarified by centrifugation at 20000*g* for 30 min and then brought to 40% saturation in ammonium sulfate. The solution was centrifuged as described above, the pellet discarded, and the supernatant brought to 100% saturation in ammonium sulfate. After centrifugation as above, the pellet was dissolved in a minimum amount of 50 mM Tris buffer (buffer A) containing 1 mM $CaCl_2$ (pH 7.5) and dialyzed vs. 10 L of the same buffer with one change. The dialyzate was applied to a phenyl–Sepharose (Sigma) column and washed with 200 mL of buffer A followed by buffer A containing 0.5 M NaCl until the absorbance at 276 nm fell below 0.001 absorbancy unit. The CaM was eluted with buffer A containing 0.5 M NaCl and 10 mM EDTA. Fractions (6 mL) were collected and monitored for CaM by measuring the absorbance at 276 nm. The protein was lyophilized after the removal of EDTA (see below).

EDTA was removed from calmodulin in a collodian membrane apparatus (Schleicher & Schuell) with a 10000-dalton cut-off at 25 °C. The combined CaM-containing fractions were adjusted to pH 7.0 and concentrated 3-fold against buffer A. This procedure was repeated four additional times with redilution of the dialyzate before each change of external buffer. The solution was checked for EDTA by the laser spectroscopic method described below (see results). The CaM obtained ran as a single band on both denaturing and nondenaturing gels.

All chemicals were of the highest grade commercially available. Doubly distilled water that had been passed over a Chelex 100 column was used throughout. All metal ion solutions were standardized by a complexometric technique (Fritz et al., 1958). The concentration of calmodulin was determined with a molar absorbancy of $\epsilon_{276} = 3300\ M^{-1}\ cm^{-1}$ (Wang et al., 1982).

The absorption spectrum of CaM containing 2 equiv of Nd(III) (27.9 μM protein) was obtained on a Varian-cary 210 spectrophotometer. A 10-cm cell was used in order to avoid the concentration range where Ln(III)-containing samples of CaM aggregate (above 150 μM). Apo-CaM in buffer was used as the blank.

The fluorescence spectrum of CaM containing 2 equiv of Eu(III) (54 μM in protein) was obtained on a Perkin-Elmer MPF 44A spectrofluorometer equipped with a differential-corrected spectra unit. Eu(III) was excited at 395 nm (20-nm band pass) while the emission was scanned from 450 to 640 nm (4-nm band pass). The spectrum of apo-CaM under identical conditions was used as the blank.

A pulsed nitrogen laser pumped dye laser apparatus described elsewhere (Horrocks & Sudnick, 1981; Breen, 1984) was used to obtain the Ln(III) ion excitation spectra and lifetime data. The titration and spectral data were corrected for variations in laser power during the course of the experiment. The titration data were analyzed with a nonlinear least-squares regression algorithm. The lifetimes were obtained with the same algorithm developed by Marquardt (Bevington, 1964). All CaM solutions were buffered (25 mM Hepes, pH 7.0) and made 0.5 M in KCl to avoid nonspecific Ln(III) ion binding and the resulting precipitation that is observed when 0.1 M KCl is employed.

Results and Discussion

Excitation Spectroscopy of the $^7F_0 \rightarrow {}^5D_0$ Transition of Eu(III). Figure 1 shows the excitation spectra obtained as the laser is scanned through the transition region, and emission from the $^5D_0 \rightarrow {}^7F_2$ transition is monitored as a function of Eu(III) added to apo-CaM. The intensity of the peak increases as Eu(III) is added; however, disappointingly, the position and

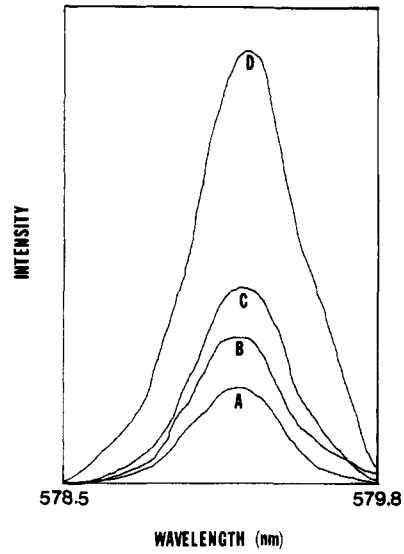

FIGURE 1: $^7F_0 \rightarrow {}^5D_0$ excitation spectra of Eu(III) bound to calmodulin (65 μM) at metal to protein ratios of (A) 0.94, (B) 1.46, (C) 1.99, and (D) 4.70.

shape of the signal vary little throughout the titration. After 2 equiv of Eu(III) has been added, the apparent maximum centers at about 579.22 nm and shifts slightly (to 579.34 nm) after the addition of 4.7 equiv. The four calcium binding sites in calmodulin are not identical and are filled in a sequential manner by lanthanide ions. Nevertheless, there is little discernible ability of the $^7F_0 \rightarrow {}^5D_0$ transition, which in principle could yield a peak at a separate position for each binding site, to distinguish amongst the sites in CaM. Two factors contribute to the lack of resolution: one is the width of the peak, which for Figure 1, trace C, is 0.53 nm or 15.9 cm^{-1} fwhm. This breadth could easily obscure differences between overlapping peaks differing by only a few tenths of a nanometer in wavelength. It has been postulated (O'Hara & Bersohn, 1982) that a heterogeneous broadening mechanism, arising from numerous local conformations around the Eu(III) in a population of protein molecules, contributes significantly to the excitation line widths in such experiments. Lowering the temperature to 77 K produces relatively little narrowing of the signal and does not resolve overlapping peaks (experiments not shown).

From an analysis of the amino acid sequence of bovine brain calmodulin, Kretsinger (1980) deduced that calcium binding sites I–IV contain three, four, three, and three potential carboxylate ligands, respectively, from aspartic or glutamic acid side chains. We recently noted (Albin & Horrocks, 1985) that there is a reasonably good correlation between the total negative charge on the ligands in the first coordination sphere of Eu(III) and the frequency of the $^7F_0 \rightarrow {}^5D_0$ transition. According to this correlation, the peak at 579.34 nm (17261 cm^{-1}) corresponds to a total ligand charge of 2.7–, consistent with the predominance of three carboxylate groups in the first coordination sphere. Considering the observed peak width and the extreme similarity of the four binding sites, it is not surprising that a resolution is not achieved in this experiment. Two sets of sites can, however, be distinguished by $^7F_0 \rightarrow {}^5D_2$ excitation spectroscopy (vide infra).

Figure 2 shows the results of titrations of apo-CaM with Eu(III) monitored by the intensity of either the $^7F_0 \rightarrow {}^5D_0$ or the $^7F_0 \rightarrow {}^5D_2$ excitation band. The interpretation of these experiments, which is supported by data obtained via tyrosine-sensitized excitation of Tb(III) (Figure 4), is as follows. Eu(III) ions titrate quantitatively into two sites as indicated

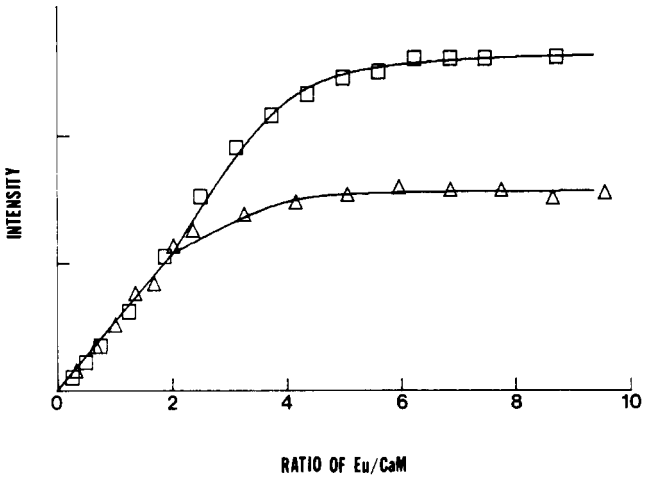

FIGURE 2: Intensity of the (λ_{ex} = 579.28 nm) $^7F_0 \rightarrow {}^5D_0$ and (λ_{ex} = 464.20) $^7F_0 \rightarrow {}^5D_2$, excitation bands ($\lambda_{em}$ = 614 nm) as a function of total equivalents of Eu(III) added to apocalmodulin (11.5 and 22.7 μM, respectively).

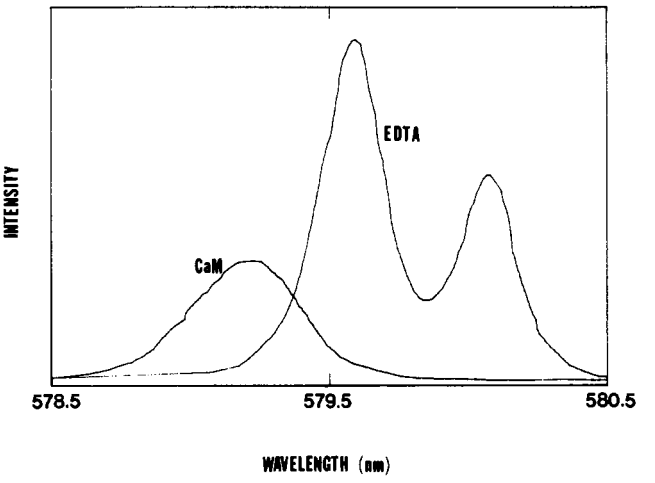

FIGURE 3: $^7F_0 \rightarrow {}^5D_0$ excitation spectra of Eu(III) (34 μM) bound to EDTA (49 μM) and calmodulin (66 μM).

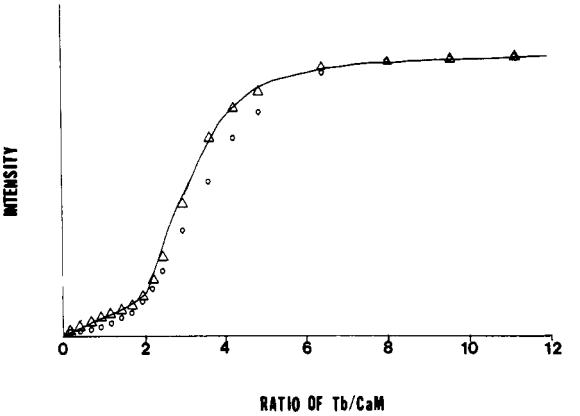

FIGURE 4: Tyrosine-sensitized Tb(III) emission at 545 nm as a function of total equivalents of Tb(III) added to apocalmodulin (10 μM) (△) and Ca(II)-bound calmodulin (10 μM) (○). In the Ca(II)-bound titration, 4 equiv of Ca(II) was added to the apocalmodulin solution.

by a straight line plot up to 2 equiv of added metal ion. The remaining sites are then filled with a dissociation constant of 2 μM (assuming two independent, equivalent sites). The solid lines are the theoretical curves corresponding to this interpretation.

The two titrations have been normalized by matching the intensities at 2 equiv of added Eu(III) ion. It is evident from this experiment that filling the second two (weaker) sites produces a greater ($^7F_0 \rightarrow {}^5D_0$) or lesser ($^7F_0 \rightarrow {}^5D_2$) intensity in the excitation signal than that caused by filling the first two (tight) sites. In the $^7F_0 \rightarrow {}^5D_0$ case, this is probably due to the fact that Eu(III) ions in the second two sites absorb more strongly than those in the first two sites, perhaps as a result of a more distorted ligand field. In the $^7F_0 \rightarrow {}^5D_2$ case, the difference is due to selective excitation of Eu(III) in the tight sites by judicious selection of the excitation wavelength (see Figure 7).

It should be noted that $^7F_0 \rightarrow {}^5D_0$ excitation spectroscopy of Eu(III) provides a general and extremely sensitive method for analyzing for contaminating levels of EDTA or EGTA in biochemical samples. This is particularly useful for checking the purity of proteins, such as CaM, where EDTA or EGTA is necessary in the isolation and purification of the macromolecule. It is our experience, even when dialysis or chromatographic procedures have been carried out in an effort to remove EDTA or EGTA, that significant levels of the chelating agent often remain. Indeed, we have found commercial CaM (Sigma) to be contaminated with EGTA. Excitation spectroscopy allows a rapid and unambiguous quantitation of EDTA levels in a sample and does not, of course, involve the use of radioactive tracers.

Figure 3 shows a superposition of the excitation spectra of CaM and EDTA when each is present in excess of the same concentration of Eu(III). It can be seen that the two-peaked spectrum of $EuEDTA^-$ is clearly distinguishable from Eu(III) bound to CaM and, in fact, dominates a spectrum containing both species at the same concentration. The concentration of EDTA in a sample is determined by the following procedure. The emission intensity of a sample containing an excess of $EuCl_3$ is first measured while exciting at 580.1 nm [to eliminate interference from protein-bound Eu(III); see Figure 3]; then, a known amount of EDTA is added, and the intensity is remeasured. This provides information sufficient to calculate the concentration of EDTA originally present in the sample. Using this procedure, we have been able to measure concentrations of EDTA as low as 0.2 μM in a CaM solution.

Binding of Tb(III) to CaM by Tyrosine-Sensitized Luminescence and Laser Excitation of the $^5D_4$ Level. Three laboratories have reported on the binding of Tb(III) to CaM by monitoring the sensitized emission of Tb(III) at 545 nm as the protein is irradiated at 280 nm in the tyrosine absorption band. Wang et al. (1982) and Kilhoffer et al. (1980) noted that the addition of the first 2 equiv of Tb(III) produces very little sensitized emission, while a large increase in this quantity is observed as Tb(III) is added beyond 2 equiv. In contrast, Wallace et al. (1982) report that the first equivalent of Tb(III) exhibits very little sensitized luminescence, the second and third equivalents are sensitized to a large extent, and the fourth equivalent is, again, only weakly sensitized to emit. We repeated this experiment as shown in Figure 4 with results in good agreement with those of Wang et al. (1982) and Kilhoffer et al. (1980). The first 2 equiv of added Tb(III) appear to bind quantitatively, but with minimal sensitization. As additional equivalents of TbIII) are added, considerable sensitized emission is observed, which can be fit to a binding curve (two equivalent, independent sites) with a K_d of 2 μM as shown by the solid curve in Figure 4.

When the same titration was carried out in the presence of Ca(II) (present at 4 times the CaM concentration), the first 2 equiv of Tb(III) again appear to bind quantitatively (Figure 4). They are sensitized to a slightly lesser degree, perhaps due to the fact that the protein is in a different conformation owing to occupancy of the remaining binding sites by Ca(II). Upon

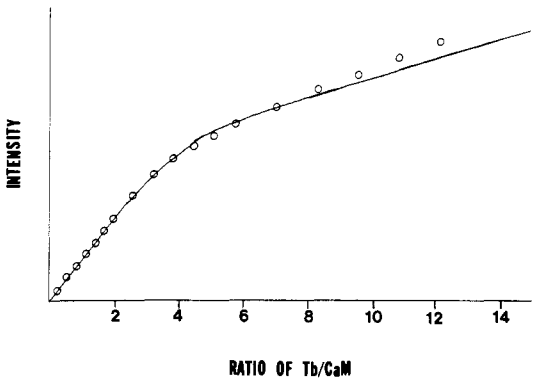

FIGURE 5: Tb(II) emission at 545 nm as a function of total equivalents of Tb(III) added to apocalmodulin (15 μM) (λ_{ex} = 488 nm).

addition of Tb(III) beyond 2 equiv in the presence of Ca(II), the sensitized emission rises somewhat more slowly owing to a competition for the two weaker sites between the two types of ion. The final level of sensitized Tb(III) luminescence is the same as for the titration in the absence of Ca(II), proving full occupancy of the four binding sites by Tb(III) in the presence of this level of Ca(II).

An analogous titration was carried out by monitoring 545-nm emission as the Tb(III) was directly excited to the $^5D_4$ state by light from the pulsed dye laser at 488 nm. This titration curve is shown in Figure 5 with the solid curve representing quantitative binding of Tb(III) to two tight sites followed by a binding curve for independent binding to two weaker sites with a K_d of 3 μM. The good agreement between the K_d values for the two Tb(III) titrations and the Eu(III) titration supports the interpretation that under the high ionic strength conditions employed (0.5 M KCl) these Ln(III) ions bind quantitatively to two tight sites followed by weaker binding to two other sites. The failure of this curve to level off at higher concentrations of added Tb(III) is due to the signal from unbound Tb(III). This contribution was determined independently (16% of signal at 9.4 equiv) and allowed for in the curve describing the theoretical fit.

The sensitized emission arises from a nonradiative energy transfer between thee two tyrosine residues and the bound Tb(III) ions. The titration results thus imply that the tight binding sites, which are only feebly sensitized, are remote from the two tyrosine moieties in the molecule. Since the latter occur at positions 99 and 138 of the polypeptide sequence in calcium binding domains III and IV of the protein, the tight sites initially occupied by Tb(III) are sites I and II, in accord with the conclusions of others (Kilhoffer et al., 1980; Wang et al., 1982).

Relative Binding across the Lanthanide Ion Series. For a simple metal ion chelating ligand we have recently shown (Albin et al., 1984) that $^7F_0 \rightarrow {}^5D_0$ excitation spectroscopy of Eu(III) can be used in conjunction with metal ion competition experiments to determine the relative binding constants of all the Ln(III) ions across the series toward this ligand. For a simple ligand or protein with a single metal ion binding site, the ratio of dissociation constants, K_d^{Eu}/K_d^{Ln}, is

$$\frac{K_d^{Eu}}{K_d^{Ln}} = \frac{[Eu]_t - [Eu]_b}{[Ln]_t - [Ln]_b}\frac{[Ln]_b}{[Eu]_b} \qquad (1)$$

where the subscripts t and b represent total and bound concentrations, respectively. In a case, such as CaM, where there is more than one nonequivalent site with differing dissociation constants and differing spectroscopic properties, a rigorous quantitative determination of all the relative binding constants is not possible. We have recently shown (Breen et al., 1985a,b)

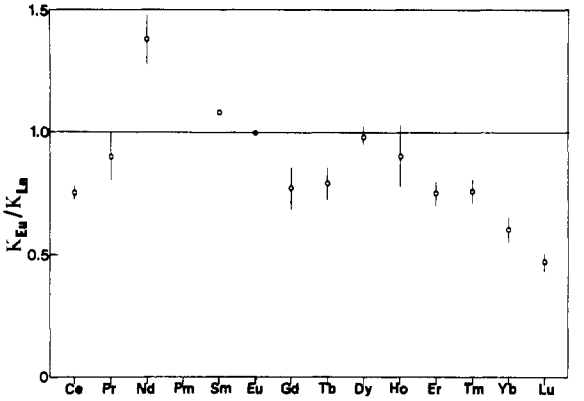

FIGURE 6: Relative binding affinities of Eu(III) and the Ln(III) ions for calmodulin (10 μM) as determined from metal ion competition experiments (see text).

in the case of parvalbumin (two nonequivalent binding sites, virtually identical spectroscopic properties) that treatment of the two sites as equivalent produces a K_d^{Eu}/K_d^{Ln} ratio closely approximating the average of the ratios for the two sites. For CaM, where we treat the four sites as equivalent as one must in this type of analysis, the relationship of the result to the actual dissociation constant ratios is even less clear. Nevertheless, the present experiment, wherein a CaM (10 μM) molecule is confronted with 6 equiv of Eu(III) and 6 equiv of a competing Ln(III) ion, yields some idea of the relative overall affinities of the protein for the various ions. In our treatment, the intensity of the $^7F_0 \rightarrow {}^5D_0$ excitation peak of CaM to which 6 equiv of Eu(III) has been added is taken (Figure 2) as 0.86 of the intensity for occupation of all four sites by Eu(III). The measured intensity is directly proportional to the concentration of bound Eu(III). By use of this procedure, the values of "K_d^{Eu}/K_d^{Ln}" plotted in Figure 6 were obtained. A value greater the 1.0 implies that the particular Ln(III) ion binds more strongly than Eu(III). While the observed trend is by no means smooth across the series, the most evident feature is the decrease in affinity for Ln(III) ions at the end of the series. The highest affinity appears to be for Nd(III), and while it may be a coincidence, of all the Ln(III) ions its ionic radius most nearly matches that of Ca(II). A decrease in affinity for the later members of the series was also observed in the case of parvalbumin (Breen, 1984; Breen et al., 1985a,b). It may be that this behavior is a general characteristic of the helix–loop–helix binding sites in calcium-modulated proteins (Kretsinger, 1980).

Excitation Spectroscopy of the $^7F_0 \rightarrow {}^5D_2$ Transition of Eu(III). In contrast to the $^7F_0 \rightarrow {}^5D_0$ transition between nondegenerate levels, excitation spectroscopy of the higher lying $^5D_1$ and $^5D_2$ states reveals details of the ligand field splittings of these levels, even when only a single metal ion environment is involved. For Eu(III) in a single, low-symmetry binding site the $^5D_1$ and $^5D_2$ levels can be expected to be split into three and five components, respectively. Scanning the laser through either of these regions reveals this splitting. Ions in the $^5D_1$ and $^5D_2$ states undergo a very rapid radiationless deexcitation to the long-lived $^5D_0$ level from which emission occurs. Excited-state lifetimes measured upon excitation into the higher levels are identical with that of the $^5D_0$ state. In the case of CaM, $^7F_0 \rightarrow {}^5D_0$ excitation spectroscopy failed to resolve frequency differences amongst the four calcium binding sites. We therefore explored the excitation spectroscopy of the higher lying levels in the anticipation that differences in the ligand field splittings among the sites would allow their resolution. Such resolution was achieved in some measure for

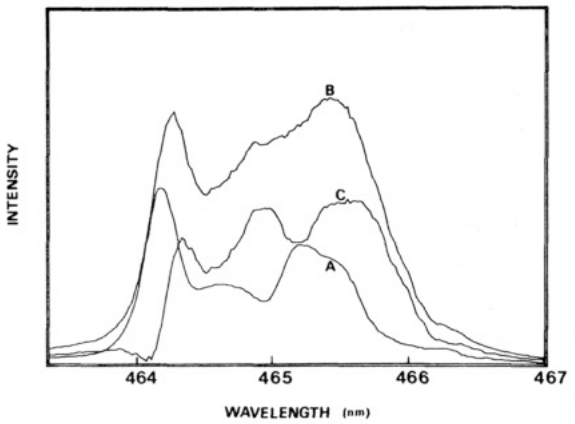

FIGURE 7: $^7F_0 \rightarrow {}^5D_2$ excitation spectra of Eu(III) bound to apocalmodulin (10 μM) at metal to protein ratios of (A) 2.0 and (B) 6.0, and (C) the difference spectrum obtained by subtracting spectrum A from spectrum B.

the $^7F_0 \rightarrow {}^5D_2$ transition. A whole series of excitation spectra for this transition were recorded as Eu(III) was added to apo-CaM. No change in the overall shape of the spectra was noticed until after 2 equiv of metal ion had been added. Subsequent additions of Eu(III), however, produced quite significant changes in the overall shape. Figure 7 shows the excitation spectra for apo-CaM (77 μM) to which 2.0 (A), and 6.0 (B) equiv of Eu(III) had been added. These two traces represent the spectra for occupancy of the first two tight sites alone and for complete occupancy of all four sites. The two spectra clearly differ with respect to structure as well as amplitude, consistent with sequential occupation of nonequivalent sites. The difference spectrum C obtained by subtracting spectrum A from spectrum B represents the spectrum for occcupation of the two weaker sites alone. This difference spectrum (full occupancy minus the first two equivalents) shows that, by judicious choice of excitation wavelength, site-selective experiments can be carried out even when all sites are occupied. For instance, irradiation at 464.2 nm will excite ions in the tight sites almost exclusively, while laser light of 465.7 nm will predominantly excite ions in the weaker sites. Potential differences in lifetimes and emission spectra between classes of site can be revealed by this site-selective technique. Another area where spectra of this type should prove valuable is in metal ion competition experiments wherein the sites from which Eu(III) is preferentially displaced can be determined. As a practical matter, the $^7F_0 \rightarrow {}^5D_2$ transition is useful because it is more than 10 times stronger in absorption than the $^7F_0 \rightarrow {}^5D_0$ transition, significantly shortening the signal averaging time necessary to obtain a good signal to noise ratio and leading to higher quality data.

Determination of the Number of Water Molecules Coordinated to Eu(III) Bound to CaM. The coordination of Eu(III) to the Ca(II) ion binding sites of CaM can be further characterized by means of the reciprocal excited-state lifetimes measured separately in H_2O and D_2O solution. We have shown (Horrocks & Sudnick, 1979) that the number of water molecules, q, coordinated to Eu(III) is

$$q = 1.05(\tau_{H_2O}^{-1} - \tau_{D_2O}^{-1}) \quad (2)$$

where τ^{-1} is the reciprocal of the excited-state lifetime in the solvent indicated. The measured $\tau_{H_2O}^{-1}$ values were 2.47, 2.43, and 2.57 ms^{-1} for addition of 1, 2 and 4 equiv of Eu(III), respectively, to apo-CaM. The corresponding $\tau_{D_2O}^{-1}$ values were respectively 0.44, 0.47, and 0.53 ms^{-1}. Application of eq 2 leads to the result that 2.1, 2.0, and 2.1 water molecules are coordinated to the Eu(III), on average, for the respective degrees of loading of CaM with Eu(III). This finding suggests that two water molecules are coordinated at each of the four sites. Since the total coordination number of a Ln(III) ion bound at a Ca(II) ion site in a protein is expected to be in the 6–8 range (Horrocks, 1982), our measurement implies that the protein supplies at least four liganding groups at each coordination site, and perhaps more. Since there are three, and in one case four, potential carboxylate ligands in each of the putative binding loops (Kretsinger, 1980), it is likely that these as well as one or more backbone peptide carbonyl groups constitute the ligating moieties. Having four or more liganding groups participate in the metal ion coordination is consistent with the relatively tight binding observed.

Förster-Type Nonradiative Energy-Transfer Distance Measurement between Eu(III) and Nd(III) in the Two Tight Sites. In order to further characterize calmodulin structurally, we have carried out energy-transfer distance measurements between an energy donor ion, Eu(III), and an energy acceptor ion, Nd(III), employing some refinements over our previously described procedures (Horrocks et al., 1980, 1983; Rhee et al., 1981; Snyder et al., 1981). Since calmodulin binds the first two equivalents of added Ln(III) ions quantitatively, we have restricted our distance measurements to calmodulin to which a 19:1 ratio of Nd(III) to Eu(III) has been added to a total of 2 equiv. The preponderance of Nd(III) ensures that virtually every Eu(III) ion will have a Nd(III) neighbor. We have attempted to achieve the most reliable distance estimate possible by minimizing the assumptions made when evaluating the parameters of Förster's equation and by using luminescence lifetime data analyzed by a computer that has been directly interfaced to our signal averager. In addition, we have also carried out parallel, independent measurements in H_2O and D_2O solution and obtained good agreement between the results of the two experiments.

The following four parameters are involved in the calculation of the critical distance parameters, R_0, of Förster's equation (eq 3): κ^2, the orientation factor; n^{-4}, the dielectric constant

$$R_0^6 = (8.78 \times 10^{-25})\kappa^2\phi n^{-4}J \quad (3)$$

factor; ϕ, the quantum yield in the absence of energy transfer; J, the spectral overlap integral between the emission spectrum of the energy donor and the absorption spectrum of the energy acceptor. For reasons set out in our earlier papers, we take κ^2 as 2/3 and n as 1.35. The spectral overlap integral has the form of eq 4, where $F(\nu)$ is the luminescence emission spectrum

$$J = \int F(\nu)\epsilon(\nu)\nu^{-4}\,d\nu / \int F(\nu)\,d\nu \quad (4)$$

of the energy donor, $\epsilon(\nu)$ is the absorption spectrum of the energy acceptor, and ν is the frequency (cm^{-1}). In the past we have had to rely on the absorption spectra of model complexes for $\epsilon(\nu)$; however, we have now measured the absorption spectrum of Nd(III) ions in the two tight sites of calmodulin (Figure 8). These data, along with the corrected emission spectrum of Eu(III) bound to calmodulin (Figure 8), allow us to calculate a realistic value of J, in this case 1.40×10^{-17} cm^6 mol^{-1}. The measured luminescence lifetimes are $\tau_0^{H_2O} = 427.2$ μs, $\tau_{Nd}^{H_2O} = 373.5$ μs, $\tau_0^{D_2O} = 2128$ μs, and $\tau_{Nd}^{D_2O} = 1286$ μs, where τ_0 refers to the Eu(III) excited-state lifetime in the absence of Nd(III) in the adjacent site. These values lead to efficiencies, $E = 1 - \tau_{Nd}/\tau_0$, of 0.126 and 0.396 in H_2O and D_2O, respectively. The only remaining parameter necessary to measuring the distance, r (eq 5), are the quantum

$$r = R_0[(1 - E)/E]^{1/6} \quad (5)$$

yields, ϕ^{H_2O} or ϕ^{D_2O}, for Eu(III) in the absence of energy transfer. These parameters cannot be measured because to

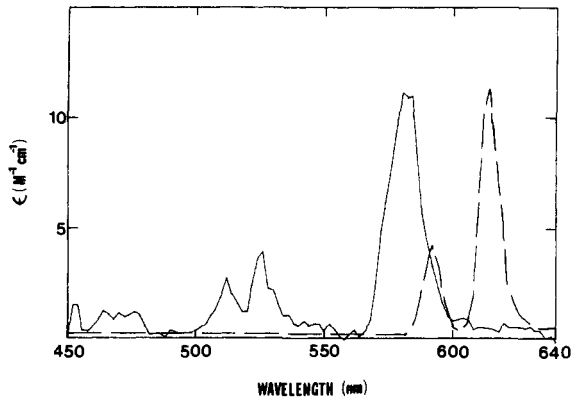

FIGURE 8: Corrected emission spectrum of Eu(III) bound to calmodulin (dashed line) (λ_{ex} = 395 nm) and the absorption spectrum of Nd(III) bound to calmodulin (solid line) on a per mole or Nd(III) basis.

Table I: Effect of Quantum Yield, ϕ, on the Critical Distance, R_0, and the Distance between Binding Sites, r

ϕ		R_0 (Å)		r (Å)	
H_2O	D_2O	H_2O	D_2O	H_2O	D_2O
0.20	1.00	8.9	11.6	12.3	12.5
0.18	0.90	8.7	11.4	12.1	12.3
0.16	0.80	8.6	11.2	11.8	12.0
0.14	0.70	8.4	11.0	11.6	11.8

do so would require the measurement of the absorption corresponding to the $^7F_0 \rightarrow {}^5D_0$ transition of Eu(III) bound to calmodulin. Owing to the forbidden nature of this transition ($\epsilon \simeq 0.05$ M^{-1} cm^{-1}), this measurement is clearly impossible. The ratio of τ_0 values in H_2O and D_2O does, however, yield the ϕ^{H_2O}/ϕ^{D_2O} quotient, 0.20. Table I shows the effect of various assumptions regarding the value of ϕ^{D_2O} on the final estimate of the distance between the two tight sites. The quantum yield of the Eu(III) aqua ion in D_2O solution has been reported to be 0.78 (Stein & Wurzberg, 1975), suggesting that the ϕ^{D_2O} values listed in Table I are reasonable. It should be noted that the independent H_2O and D_2O measurements are in excellent agreement with one another, even though the R_0 values and measured efficiencies are quite different. Taking these findings into account, a reasonable distance estimate would be $r = 12.1 \pm 0.5$ Å. This value is very close to the distance of 11.8 Å measured by X-ray crystallography between the CD and EF calcium binding sites in parvalbumin and strongly supports the postulate (Kretsinger & Barry, 1975; Kretsinger, 1980) that the calmodulin structure consists of two pairs of EF hand domains, each pair being very similar to those found in parvalbumin.

The protocol, introduced here, of carrying out simultaneous distance measurements in H_2O and D_2O and of evaluating spectral overlap integrals directly from absorption spectra of metal ions bound to the protein in question should increase the reliability of distance measurements of this type.

Conclusions

CaM binds Ln(III) ions initially at two tight binding sites in domains I and II of the protein and subsequently at two more weakly binding sites in domains III and IV. This is evidenced by the strong tyrosine-sensitized luminescence of Tb(III) binding to the weaker sites and by significant differences in the structures of the $^7F_0 \rightarrow {}^5D_2$ excitation spectra of Eu(III) ions as the two classes of sites are filled. A study of $^7F_0 \rightarrow {}^5D_2$ excitation spectra under carefully controlled conditions in metal ion competition experiments should resolve the question of whether or not Ca(II) binds to CaM in the same sequence as does Tb(III). A decrease in the affinities of Ln(III) ions late in the series for CaM as compared with Eu(III) is observed, analogous to that found for parvalbumin. It may be that this behavior is a general characteristic of "EF-hand"-containing calcium-modulated proteins. The finding that there are two water molecules coordinated to Eu(III) at each of the four sites in CaM, whereas our earlier study (Rhee et al., 1981) revealed only one water molecule at each site in parvalbumin, is consistent with the higher degree of ligation and the observed tighter binding of metal ions by the latter protein.

The determination of distance by parallel measurements of inter metal ion Förster-type energy transfer separately in H_2O and D_2O solution provides a means of assessing the internal consistency of the results. In the present measurement of the distance between the two tight binding sites of CaM, the actual absorption spectrum of the acceptor ion, Nd(III), bound to the sites in question, was used in evaluating the spectral overlap integral. These procedures provide the most reliable distance estimates possible within the limits of validity of Förster's theory as applied to metal ions in proteins. The distance we observe is consistent with the postulate that the structure of CaM is homologous to that of parvalbumin.

Registry No. Eu, 7440-53-1; Tb, 7440-27-9; Nd, 7440-00-8; Ce, 7440-45-1; Pr, 7440-10-0; Sm, 7440-19-9; Gd, 7440-54-2; Dy, 7429-91-6; Ho, 7440-60-0; Er, 7440-52-0; Tm, 7440-30-4; Yb, 7440-64-4; Lu, 7439-94-3; EDTA, 60-00-4; EGTA, 67-42-5.

References

Albin, M., & Horrocks, W. D., Jr. (1985) *Inorg. Chem. 24*, 895–900.

Albin, M., Farber, G. K., & Horrocks, W. D., Jr. (1984) *Inorg. Chem. 23*, 1648–1651.

Andersson, T., Drakenberg, T., Forsén, S., & Thulin, E. (1982) *Eur. J. Biochem. 126*, 501–505.

Andersson, A., Drakenberg, T., Thulin, E., & Forsén, S. (1983a) *Eur. J. Biochem. 134*, 459–465.

Andersson, A., Forsén, S., Thulin, E., & Vogel, H. J. (1983b) *Biochemistry 22*, 2309–2313.

Bevington, P. R. (1969) *Data Reduction and Error Analysis for the Physical Sciences*, pp 235–246, McGraw-Hill, New York.

Breen, P. J. (1984) Ph.D. Thesis, The Pennsylvania State University.

Breen, P. J., Hild, E. K., & Horrocks, W. D., Jr. (1985a) *Biochemistry 24*, 4991–4997.

Breen, P. J., Johnson, K. A., & Horrocks, W. D., Jr. (1985b) *Biochemistry 24*, 4997–5004.

Burger, D., Stern, E. A., & Cox, J. A. (1983) *J. Biol. Chem. 258*, 14733–14739.

Cheung, W. Y. (1980a) *Science (Washington, D.C.) 207*, 19–27.

Cheung, W. Y., Ed. (1980b) *Calcium and Cell Function*, Vol. 1, Academic Press, New York.

Cormier, M. J. (1983) in *Calcium in Biology* (Spiro, T. G., Ed.) pp 53–106, Wiley, New York.

Cox, J. A. (1984) *Fed. Proc., Fed. Am. Soc. Exp. Biol. 43*, 3000–3004.

Cox, J. A., Malnöe, A., & Stern, E. A. (1981) *J. Biol. Chem. 256*, 3218–3222.

Dedman, J. R., & Kaetzel, M. A. (1983) *Methods Enzymol. 102G*, 1–8.

Forsén, S., Thulin, E., Drakenberg, T., Krebs, J., & Seamon, K. (1980) *FEBS Lett. 117*, 189–94.

Fritz, J. S., Oliver, R. T., & Pietrzyk, D. J. (1958) *Anal. Chem. 30*, 1111–1114.

Haiech, J., Klee, C. B., & Demaille, J. G. (1981) *Biochemistry 20*, 3890–3897.
Horrocks, W. D., Jr. (1982) *Adv. Inorg. Biochem. 4*, 201–261.
Horrocks, W. D., Jr., & Sudnick, D. R. (1979) *J. Am. Chem. Soc. 101*, 334–340.
Horrocks, W. D., Jr., & Sudnick, D. R. (1981) *Acc. Chem. Res. 14*, 384–392.
Horrocks, W. D., Jr., Rhee, M. J., Snyder, A. P., & Sudnick, D. R. (1980) *J. Am. Chem. Soc. 102*, 3650–3652.
Horrocks, W. D., Jr., Mulqueen, P., Rhee, M. J., Breen, P. J., & Hild, E. K. (1983) *Inorg. Chim. Acta 79*, 24–25.
Kilhoffer, M. C., Demaille, J. G., & Gerard, D. (1980a) *FEBS Lett. 116*, 269–272.
Kilhoffer, M. C., Gerard, D., & Demaille, J. G. (1980b) *FEBS Lett. 120*, 99–103.
Klee, C. B., & Vanaman, T. C. (1982) *Adv. Protein Chem. 35*, 213–321.
Klee, C. B., Crouch, T. H., & Richman, P. G. (1980) *Annu. Rev. Biochem. 49*, 489–515.
Kohse, K. P., & Heilmeyer, L. M. G., Jr. (1981) *Eur. J. Biochem. 117*, 507–513.
Krebs, J., & Carafoli, E. (1982) *Eur. J. Biochem. 124*, 619–627.
Kretsinger, R. H. (1980) *CRC Crit. Rev. Biochem. 8*, 119–174.
Kretsinger, R. H., & Barry, C. D. (1975) *Biochim. Biophys. Acta 405*, 40.
O'Hara, P. B., & Bersohn, R. (1982) *Biochemistry 21*, 5269–5272.
Potter, J. D., Strang-Brown, P., Walker, P. L., & Iida, S. (1983) *Methods Enzymol. 102*, 135–143.
Rhee, M. J., Sudnick, D. R., Arkle, V. K., & Horrocks, W. D., Jr. (1981) *Biochemistry 20*, 3328–3334.
Seamon, K. B., & Kretsinger, R. H. (1983) in *Calcium in Biology* (Spiro, T. G., Ed.) pp 1–51, Wiley, New York.
Snyder, A. P., Sudnick, D. R., Arkle, V. K., & Horrocks, W. D., Jr. (1981) *Biochemistry 20*, 3334–3339.
Stein, G., & Würzberg, E. (1975) *J. Chem. Phys. 62*, 208–213.
Wallace, R. W., Tallant, E. A., Dockter, M. E., & Cheung, W. Y. (1982) *J. Biol. Chem. 257*, 1845–1854.
Wang, C.-L. A., Aquaron, R. R., Leavis, P. C., & Gergely, J. (1982) *Eur. J. Biochem. 124*, 7–12.

High-Resolution Proton Nuclear Magnetic Resonance Studies of the Glucocerebrosidase Activator Protein from Gaucher Spleen†

Leung Sheh‡ and Robert H. Glew*
Department of Biochemistry, University of Pittsburgh School of Medicine, Pittsburgh, Pennsylvania 15261
A. A. Bothner-By and P. K. Mishra
Department of Chemistry, Carnegie-Mellon University, Pittsburgh, Pennsylvania 15213
Received February 1, 1985

ABSTRACT: A heat-stable protein factor (HSF) obtained from the spleen of a patient with Gaucher's disease that activates glucocerebrosidase was studied by 600-MHz proton NMR spectroscopy. Assignments for a number of aromatic and aliphatic resonances were made on the basis of spin-decoupling, pH-titration, and resolution-enhancement experiments. The upfield ring current shifted aliphatic region and the downfield aromatic region were examined by nuclear Overhauser effect (NOE) methods using both pulsed Fourier-transform spectroscopy and correlation spectroscopy. It was found that a number of upfield-shifted methyl groups and certain methylene groups of specific aliphatic amino acid residues are in proximity relationships with several aromatic residues, forming a compact hydrophobic clustering site. Of special interest, tyrosine A, phenylalanine A, tryptophan B_1, and tryptophan B_2 were found to be located close to a cluster of aliphatic residues, indicating that the hydrophobic site of the HSF is conformationally rigid and its tertiary structure very compact. A two-dimensional structural model of the hydrophobic site of HSF is proposed.

Gaucher's disease is an inherited lysosomal storage disease in which glucocerebroside accumulates in mononuclear phagocytic cells of the reticuloendothelial system because of a marked deficiency of glucocerebrosidase (glucocerebroside: β-glucosidase; EC 3.2.1.45) activity (Lee, 1968; Fredrickson & Sloan, 1972; Brady & Barranger, 1983). In recent years, much effort has been devoted to improving our understanding of the regulation of the enzyme and to explaining the molecular basis of the distinction between the clinical extremes of Gaucher's disease defined at one end of the spectrum by adults with the type 1 form of the disease who live into the seventh or eighth decade of life without neurologic involvement and at the other end by infants with the type 2 form of the disease who usually die by the age of 2, always with extensive primary central nervous system dysfunction (Fredrickson & Sloan, 1972; Brady & Barranger, 1983).

The search for an explanation of the genetic diversity of Gaucher's disease has focused in part on activators of glucocerebrosidase, namely, acidic phospholipids and a heat-stable factor from spleen first described by Ho & O'Brien (1971) and later purified to homogeneity by Peters et al. (1977). Solubilized preparations of glucocerebrosidase of normal human spleen and liver (Glew et al., 1982; Basu et al., 1984; Prence et al., 1985) and rat liver (Basu & Glew, 1984) are

† This work was supported by Grant AM 31357 from the U.S. Public Health Service, National Institutes of Health. Spectra were obtained at the NMR Facility for Biomedical Studies, Pittsburgh, PA, supported by NIH Grant RR 00292.
‡ Present address: Department of Chemistry, West Virginia University, Morgantown, WV 26505.

0006-2960/85/0424-6645$01.50/0